World Journal of Advanced Research and Reviews
eISSN: 2581-9615 CODEN (USA): WJARAI
Cross Ref DOI: 10.30574/wjarr
Journal homepage: https://wjarr.com/

(RESEARCH ARTICLE)

Check for updates

Spatio-Temporal Analysis of LULC Change, UHI intensification in Ludhiana City (2001-2021)

Jashanjot Singh * and Apperdeep Kaur

Department of Geography, Faculty of Physical Sciences, Punjabi University Patiala, Punjab, 147002, India.

World Journal of Advanced Research and Reviews, 2026, 30(02), 2626-2639

Publication history: Received on 18 April 2026; revised on 26 May 2026; accepted on 28 May 2026

Article DOI: https://doi.org/10.30574/wjarr.2026.30.2.1519

Abstract

Cities have come a long way from their traditional structures of past to complex structures of today. Majority of population burden in future will be on cities as rapid urbanization is happening. Increasing urbanization has also created problems such as heat island effect responsible for elevating surface temperatures and compromising thermal comfort. This study analyses the spatio-temporal dynamics of Land Use/Land Cover (LULC), Urban Heat Island (UHI) and thermal comfort of Ludhiana city over a twenty-year period from 2001 to 2021. Ludhiana which is an important cultural and industrial hub of north India has experienced rapid urbanization and development. Using Landsat satellite imagery and indices such as Normalized Difference Vegetation Index (NDVI), Normalized Difference Built-up Index (NDBI), Land Surface Temperature (LST), with the help of Google Earth Engine for spatial processing, the study quantifies significant changes in urban morphology and thermal profiles. An attempt has been made to understand the correlation between increasing UHI with decreasing vegetation and increasing built-up. There is a case of strong correlation. Mean LST of various LULC classes were calculated and there is a trend of increasing LST among all LULC classes. Results indicate an 80.75% increase in built-up area primarily at the expense of vegetation (−82.88%) and waterbodies (−45.39%). Correspondingly, surface temperatures rose notably across all land classes, with built-up zones reaching an average LST of 41.8° C by 2021. There appears to be a case of intense UHI in the major parts of the city which is dispersed along with decrease in thermal comfort within this period. There is need of sustainable plans for LULC management, along with heat action plans so that there is a conducive environment that promotes public health, climate resilience, decision making involving various stakeholders of the city.

Keywords: GIS; Google Earth Engine; Land Use Land Cover; Land Surface Temperature; Urbanization; UHI

1. Introduction

Cities have become synonymous with human development. And their evolution has been going on for quite a long time from ancient Egyptian, Indian and other prominent civilizations to the complex urban structures we see today. The emergence of cities brought with it the process of urbanization. At its core, urbanization describes not only the rising number of people living in urban areas, but also the shift from rural, agrarian communities to ones characterized by service-oriented and industrial employment and lifestyles (Sharma, 2003). Urbanization has provided immense benefits to mankind such as facilitation and sharing of knowledge, beliefs, and ideas as well as elevated standard of living.

But urbanization has come at the cost of degrading the natural environment, including deforestation, increased concrete construction, and the conversion of agricultural lands into residential zones (Lwasa, 2022). Since 1990, there has been fourfold increase of population living in urban areas and in 2050, it is projected that two-thirds of the world population will be living in urban areas (Gu, 2019). In recent decades, there are common problems facing cities and their urban

* Corresponding author: Jashanjot Singh

environs such as Urban Heat Island (UHI) effects (Phelan et al., 2015). UHI is defined as contrast in temperatures of built-up and its surrounding environments. Built-up areas are known for elevated temperatures whereas waterbodies and vegetation tend to have cooler temperatures. UHI is created by combination of factors such as heat produced by humans, poor air circulation, air pollution, meteorological conditions prevalent in the city and its surrounding environments (Tzavali, 2015). As UHI of the city intensifies there is an elevation of average surface temperatures therefore creating a condition that becomes unbearable to live in.

Recently there has been significant advancement in remote sensing capabilities to map thermal flow dynamics of a region with the help of thermal satellite imageries, though there are certain limitations such as coarser resolutions, sensor calibrations, atmospheric disturbances, and image processing (Ma et al., 2021; Wu et al., 2021). There are numerous studies that have demonstrated how it can be helpful in studying urbanization and its impact on natural environments (Waleed and Sajjad, 2023; Guha et al., 2018). Cloud computing platforms such as google earth engine along with traditional software's like QGIS, ArcGIS have widened the scope of such studies. Cloud computing involves large amounts of spatial analysis on host server without the need to download or store files on personal computers (Gorelick et al., 2017)

Therefore, making it an important topic for creating sustainable and healthy habitats without compromising natural ecosystems. This study tries to understand Land Use Land Cover (LULC) and UHI dynamics correlated with deteriorating vegetation, open spaces and increasing concretization in Ludhiana city.

2. Materials and Methods

Research methodology involves data acquisition, LULC classification, assessment of LULC changes, Land Surface Temperature (LST) computation and estimation of UHI using google earth engine. Landsat imagery served as the primary data source for this study. Landsat 7 Enhanced Thematic Mapper Plus (ETM+), Landsat 8 Operational Land Imager/Thermal Infrared Sensor (OLI/TIRS) tier-1 Surface Reflectance (SR) datasets were accessed via the Google Earth Engine catalogue for the summer months (May to September) in 2001 and 2021, respectively. For land surface temperature (LST) computations, thermal bands were selected specifically for their reliability and accuracy: band 6 for Landsat 7 and band 10 for Landsat 8, following established standards in the literature. Although Landsat 8 offers two thermal bands, band 10 was favoured over band 11 due to its demonstrated consistency and better performance in LST retrieval (Jiménez-Muñoz et al., 2014; Zhou et al., 2018). Satellites, period of imagery, band used and notes are mentioned in table 1.

Support Vector Machine (SVM) was employed for supervised LULC classification, as it is known to show robust results with better boundary separation among classes with limited possible samples (Huang et al., 2002; Khatri et al., 2025). After LULC classification, accuracy assessment was done using indices such as Overall Accuracy and Kappa Coefficient (Waleed & Sajjad, 2021; Waleed & Sajjad, 2023). Normalized Difference Vegetation Index (NDVI), Normalized Difference Built-up Index (NDBI) were also calculated. Shapefiles were obtained from the Survey of India, and the Ludhiana city boundary shapefile was digitized using data from the Municipal Corporation of Ludhiana's website. QGIS software was utilized for the visualization and analysis of the maps.

Since we are using Landsat Surface Reflectance for both Landsat 7 and 8, we do not need to convert digital numbers into radiance values as it is already adjusted with atmospheric, radiometric, and geometric corrections (USGS, n.d.; Abd et al., 2025). However, to make something of a meaningful observation there is a need to apply scaling factor (USGS, n.d.; Abd et al., 2025), it is provided in Equation (1). At sensor brightness temperature is measured with the help of equation (2) along with default Fahrenheit units converted into degree Celsius (Chander et al., 2009; Waleed & Sajjad., 2023). Digital Numbers into LST have been computed using equations (3-5) as done in previous studies (Weng et al., 2003; Chander et al., 2009; Tariq et al., 2021; Waleed & Sajjad., 2023).

$$\text{ReflectanceB} = (\text{DN} \times \text{Scaling Factor}) + \text{Offset} \quad (1)$$

Scaling factor is applied to each individual pixel and then multiplied by a gain. Value of scaling factor is 0.0000275 and offset is -0.2, these values come along with metadata files of Landsat.

$$ST_B = \frac{K_2}{lnln\left(\frac{K_1}{L_\lambda}+1\right)} - 273.15 \quad (2)$$

K1 and K2 are constant values available on the official website of United States Geological Survey (Mirza & Sajjad, 2023). STB represents at satellite brightness temperature and -273.15 is subtracted to get the value in °Celsius directly as dataset is originally in Fahrenheit.

Now we have calculated at satellite brightness temperature from equation (2), now we calculate corrected emissivity (ε), which can be calculated by NDVI's each pixel value, as shown is studies (Imran et al., 2021; Waleed & Sajjad, 2023). In equation 3, emissivity correction is applied to at sensor brightness temperature STB, then LST is calculated.

$$LST = \frac{ST_B}{1+\left(\frac{\lambda \cdot ST_B}{\rho}\right) \cdot lnln\,(\varepsilon)} \quad (3)$$

Equation 4 provides the formula for obtaining the values of normalized UHI values. Many studies have applied this technique (Waleed & Sajjad, 2023; Singh & Sharston, 2023; Khatri et al., 2025) as it helps in evaluation of inconsistent thermal areas, allowing for comparison across different time periods while reducing seasonal and even diurnal temperature inconsistency bias. Below is the equation of normalized urban heat.

$$UHIn = \frac{TS-TM}{Std} \quad (4)$$

UHIn refers to normalized UHI, Ts refers to LST, whereas Tm refers to mean LST, Std is the standard deviation LST of the study area.

Indices like NDVI and NDBI were also calculated to perform a correlation among these indices with UHI. Equation 5 and 6 represent the NDVI and NDBI formulas, respectively.

$$NDVI = \frac{NIR-Red}{NIR+Red} \quad (5)$$

$$NDBI = \frac{SWIR-NIR}{SWIR+NIR} \quad (6)$$

For obtaining NDVI formula near infrared channel (band) and red channel (band) were used. Whereas for obtaining NDBI Shortwave Infrared channel (band) and near infrared channel (band) were utilized.

Furthermore, LULC maps for the year 2001 and 2021 were prepared to better understand the inter dynamics between changing LULC and LST. Overall accuracy and Kappa coefficient were derived to measure the robustness of the LULC classification.

2.1. Study Area

The study region is Ludhiana city, which is situated in north Indian state of Punjab. It is a hub of state's business and industrial activities and quite famous for its world class quality of bicycle and hosiery products. Longitudinal and latitudinal extent of city is 75.76° east to 75.95° east, and 30.82° north to 30.95° north, respectively. According to Municipal corporation of Ludhiana it has an area of 159.7 square kilometres and has a population of approximately 1.6 million (Census of India, 2011). Fig 1 depicts the location of the study area.

Over the last few decades, the city has undergone massive transformation in terms of its LULC dynamics, with significant increase in its impervious areas. Therefore, it is important to know the extent of altered heat dynamics due to changes in LULC of the city in these last twenty years.

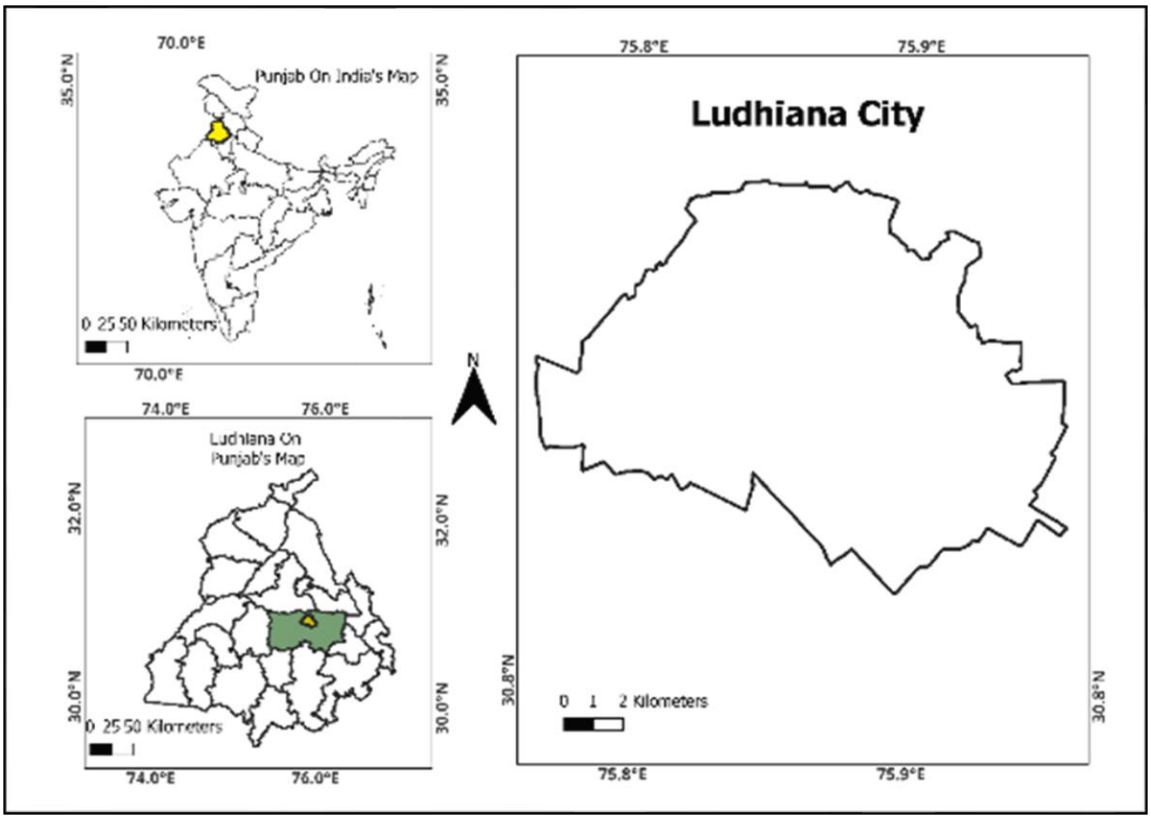

Figure 1 Location of study area

3. Results and Discussions

This section presents the key findings of the study, structured into the following components:

LULC classification with validation and accuracy assessment, Average summer temperatures and standard deviations for 2001 and 2021, Correlation between NDVI and UHI, as well as NDBI and UHI, Mean temperature variations across LULC classes over the 20-year period, and UHI spatial dynamics.

Table 1 illustrates the spatial extent of LULC classes in 2001 and 2021. In 2001, built-up areas were the largest (55.52 km^2), followed by agriculture (37.54 km^2), vegetation (36.27 km^2), barren land (20.39 km^2), and water bodies (9.98 km^2). By 2021, built-up areas expanded significantly to 100.35 km^2, while vegetation, water bodies, and barren land declined sharply. Agricultural land remained relatively stable. The table also captures percentage changes in each class over the two decades. Figure 2 visualizes the spatial distribution of LULC classes across both time periods.

Table 1 LULC Dynamics of Ludhiana city (2001-2021)

S. No	Class	Area Sq.kms (2001)	Area Sq.kms (2021)	Changes in Sq.kms	Percentage Changes in Area
1	Built-up	55.52	100.35	44.83	80.75
2	Waterbody	9.98	5.45	-4.53	-45.39
3	Vegetation	36.27	6.21	-30.06	-82.88
4	Agriculture	37.54	37.73	0.19	0.51
5	Barren land	20.39	9.96	-10.43	-51.15
	Total	159.7	159.7		

Source: Computed by Authors in Google Earth Engine

Built-up area has gained the most area in these last twenty years with a huge gain of 80.75 percent, other LULC class that has a positive gain is agricultural land, a marginal gain of 4.03 percent, other three LULC categories have negative percentage values, vegetation is among them with loss of 83.46 percent. Barren land also has loss of 51.15 percent, then waterbody with a loss of 45.39 percent (Figure 2). These findings resonate with other studies where built-up areas have expanded at the expense of reduction in vegetation and subsuming barren land areas within its fold (De La Barrera & Henríquez, 2017; Du et al., 2019; Yang et al., 2021).

Ludhiana city is no such exception in this regard with increasing population numbers and density; it has felt the same impact of transitioning from variety of landscapes to a single homogenous landscape dominated by one single LULC class, it is the built-up area. Table 2 shows the overall accuracy and kappa coefficient of LULC classification for both considered years. Overall accuracy and kappa coefficient can be considered in the category of 'substantial agreement' and the study's result can be considered for further research in this field (Rwanga and Ndambuki, 2017).

Table 2 Overall Accuracy and Kappa Coefficient of LULC Classification

Year	Overall Accuracy	Kappa Coefficient
2001	0.83	0.80
2021	0.84	0.75

Source: Computed By Authors

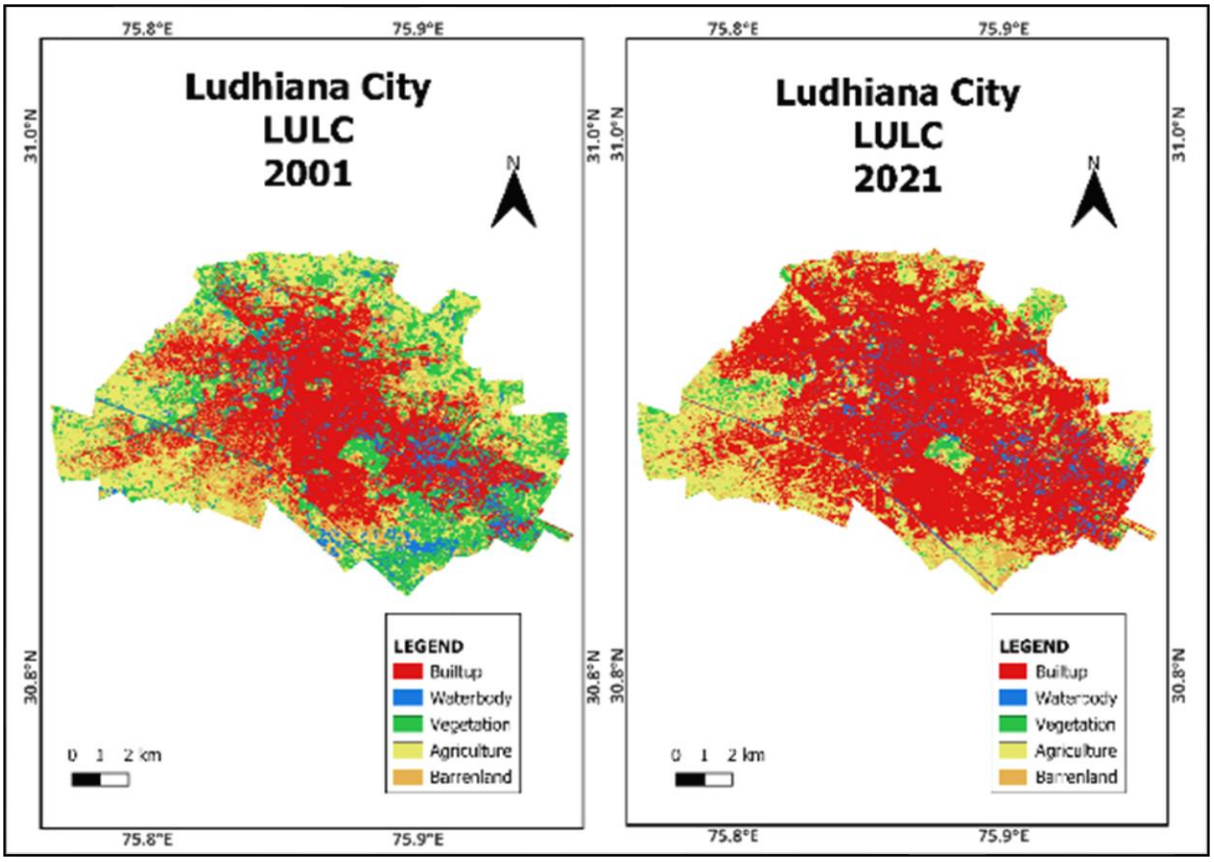

Figure 2 LULC Dynamics of Ludhiana city

Since being dominated by one single class of built-up, the average summer temperature has also increased during this time. The LST in 2001 (May to September) was 39.04° Celsius with standard deviation of 3.08° Celsius. The average maximum LST was 42.84° Celsius and average minimum LST was 35.96° Celsius. And in the year 2021, the average LST was 41.22° Celsius and standard deviation of 2.45° Celsius, the average maximum LST in 2021 was 43.67° Celsius and average minimum LST was 38.77° Celsius. Thermal changes are quite visible across this period. The more concerning fact is that changes in the average minimum LST (+2.81°) are more as compared to changes in average maximum LST

(+0.83°). Regarding changes in the LST for summer, the minimum temperature has risen form 28.81° Celsius to 30.39° Celsius from 2001 to 2021, respectively. As is the case with maximum temperature which has also risen from 41.65° Celsius to 44.08° Celsius (Figure 3).

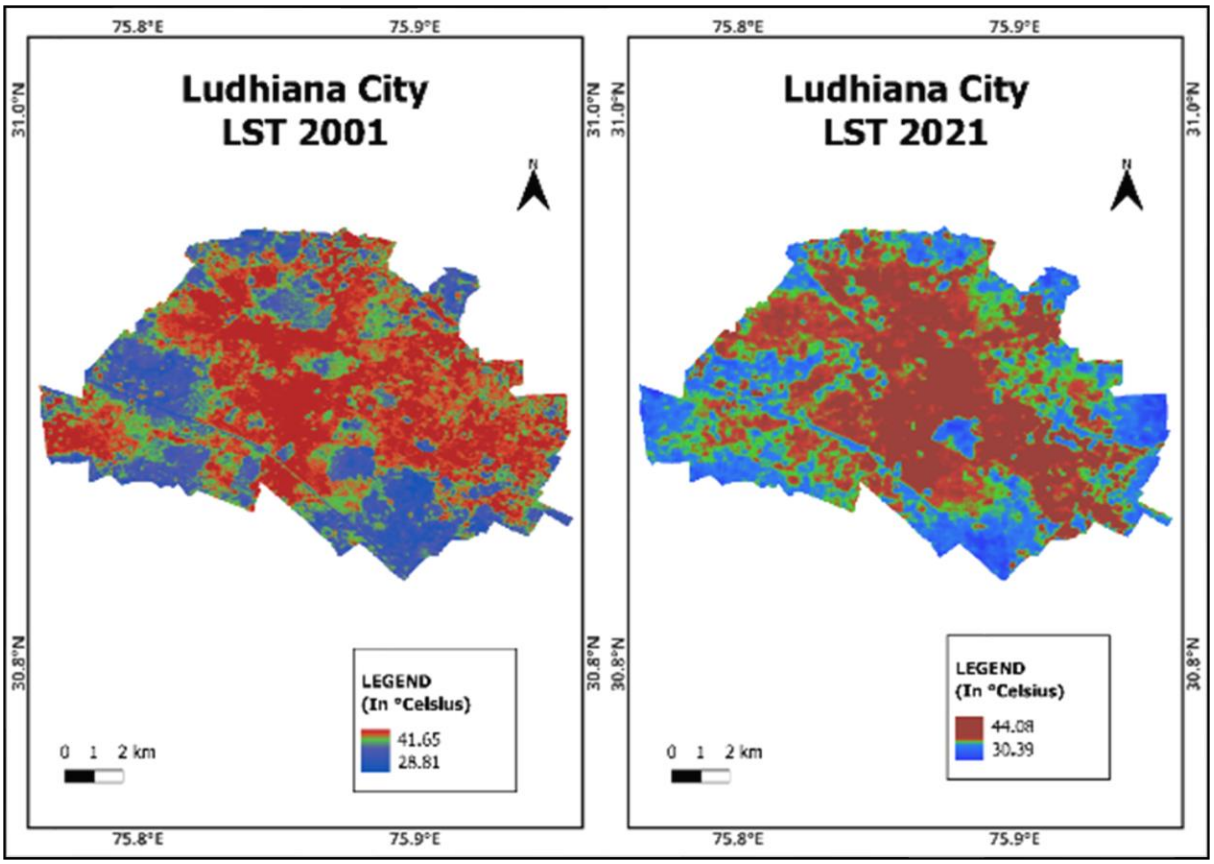

Source: QGIS and Google Earth Engine

Figure 3 LST Dynamics of Ludhiana city

We can say based on our findings that those regions of the city which had lower LST values are experiencing higher LST because of the changes in LULC dynamics, dominance of impervious surfaces (building, pavements) and vegetation loss. These findings of increase in LST and changes in LULC dynamics are consistent with our findings of increasing built-up area at the expense of vegetation loss. NDVI and NDBI are indices which are calculated with the help of satellite imageries to measure vegetation health and built-up area dynamics, respectively (Meneses-Tovar, 2011; Guha et al., 2018). NDVI (Figure 4) for the year 2001 was 0.35 which is moderate quality of vegetation and for the year 2021 it is 0.16 implying considerable degradation of vegetated surfaces (Hashim et al., 2019). So, the city has transformed from moderate vegetation health to almost negligible form of vegetation.

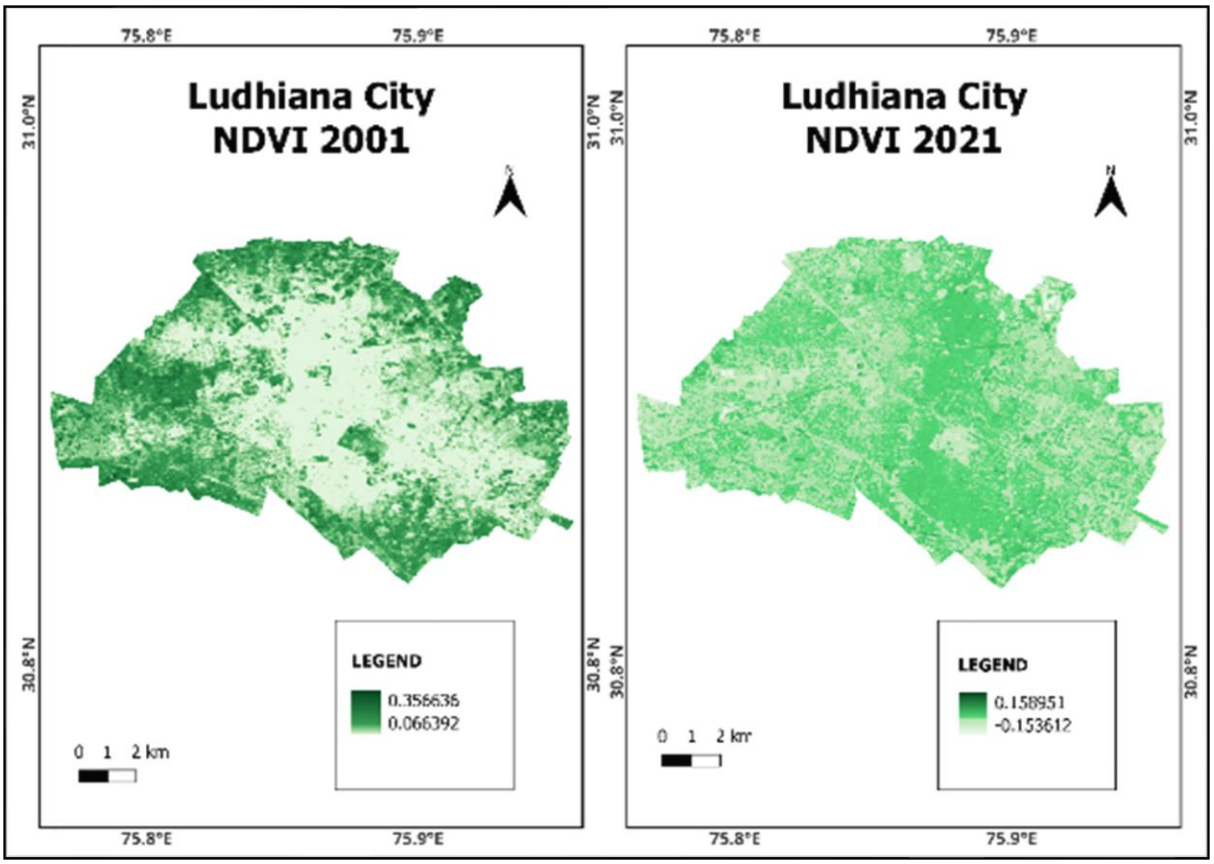

Source: QGIS and Google Earth Engine

Figure 4 NDVI of Ludhiana city

Regarding changes in the NDBI of the city, it was 0.13 in 2001 and in 2021 it had a value of 0.26. Increase in the built-up area has a positive relationship with increasing LST, as built-up areas exhibit higher temperatures as compared to non-built-up areas (Alademomi et al., 2022). Figure 5 depicts the NDBI of the Ludhiana city.

This study has also examined the Pearson Correlation between NDVI vs UHI, NDBI vs UHI, as well as mean temperature variations across LULC classes. To establish the correlation, it was important to calculate zonal statistics to help differentiate between urban and non-urban areas and these statistics were calculated in google earth engine. Our findings reveals that there is a strong negative correlation between NDVI and UHI, as observed in many studies associated with LST and UHI (Zhang et al., 2010; Ogashawara and Bastos, 2012; Ahmad et al., 2024). For 2001 and 2021, the correlation values are -0.80 and -0.96, respectively for 2001 and 2021 (Figure 6 and 7), indicating that decrease in the vegetation has resulted into stronger correlation with UHI.

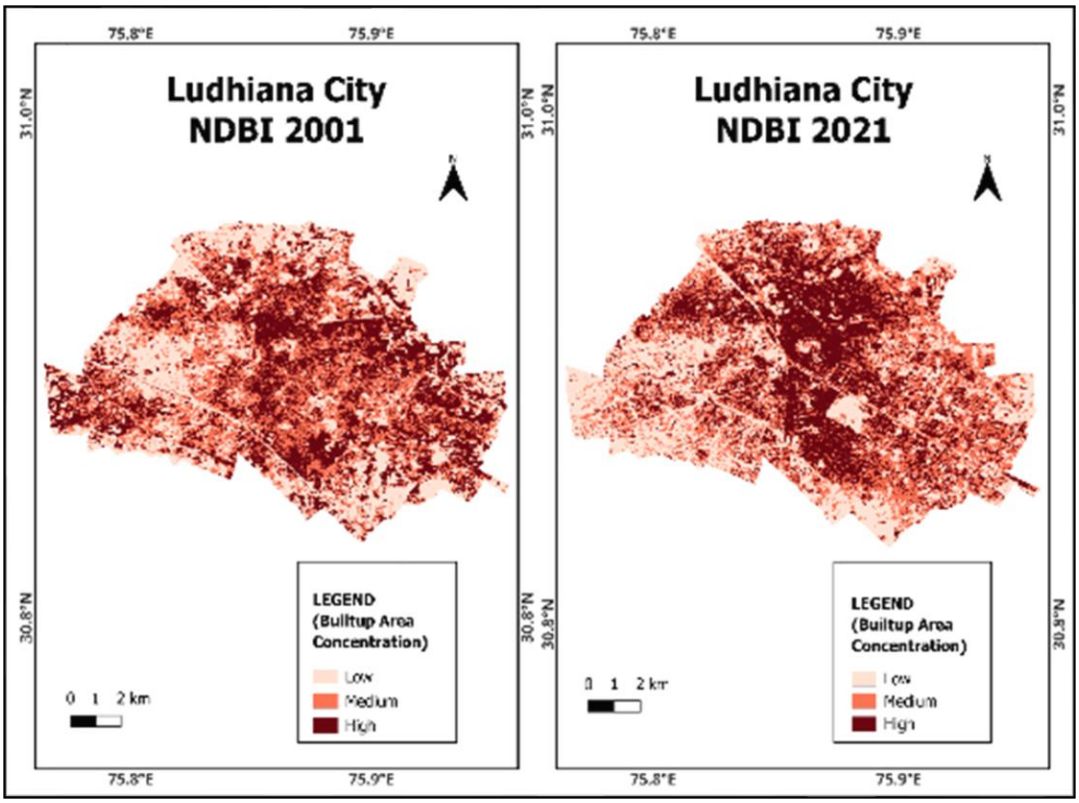

Source: QGIS and Google Earth Engine

Figure 5 NDBI of Ludhiana city

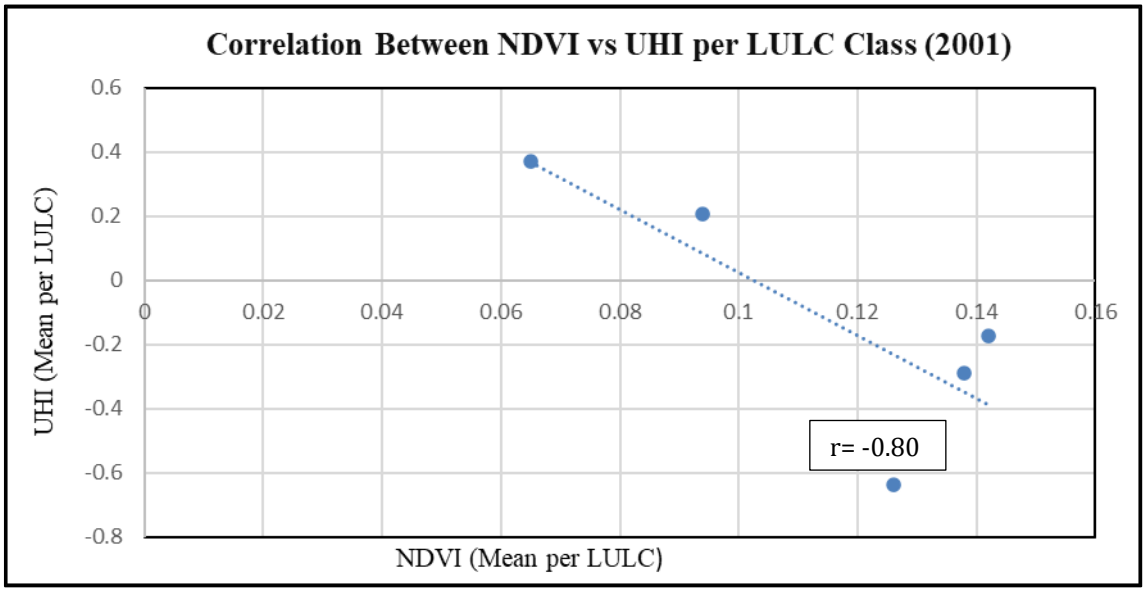

Source: Computed in Google Earth Engine

Figure 6 NDVI vs UHI Correlation for 2001

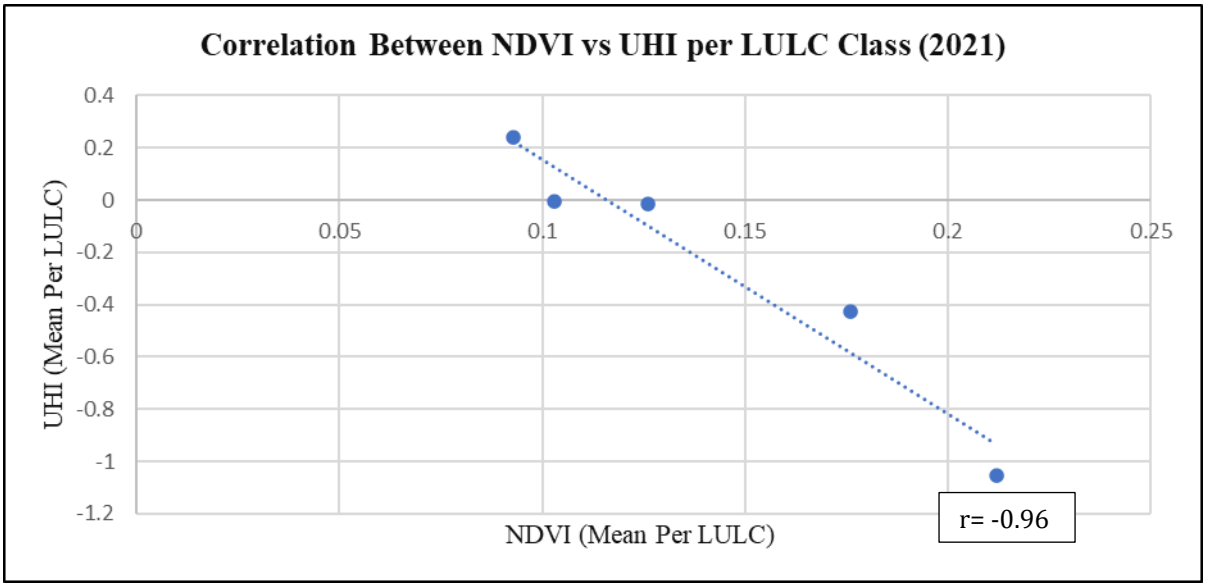

Source: Computed in Google Earth Engine

Figure 7 NDVI vs UHI Correlation for 2021

But on the other hand, NDBI and UHI tend to have a positive correlation between them (Macarof & Statescu, 2017; Singh et al., 2023) and correlation is exactly 0.95 for both years, indicating the fact that increase in built-up surroundings has resulted in intense UHI effect on the city's environment. Both indices indicate that there is a strong correlation of decrease in city's vegetation cover coupled with dominance of areas occupied by built-up structures (Figure 8 and 9).

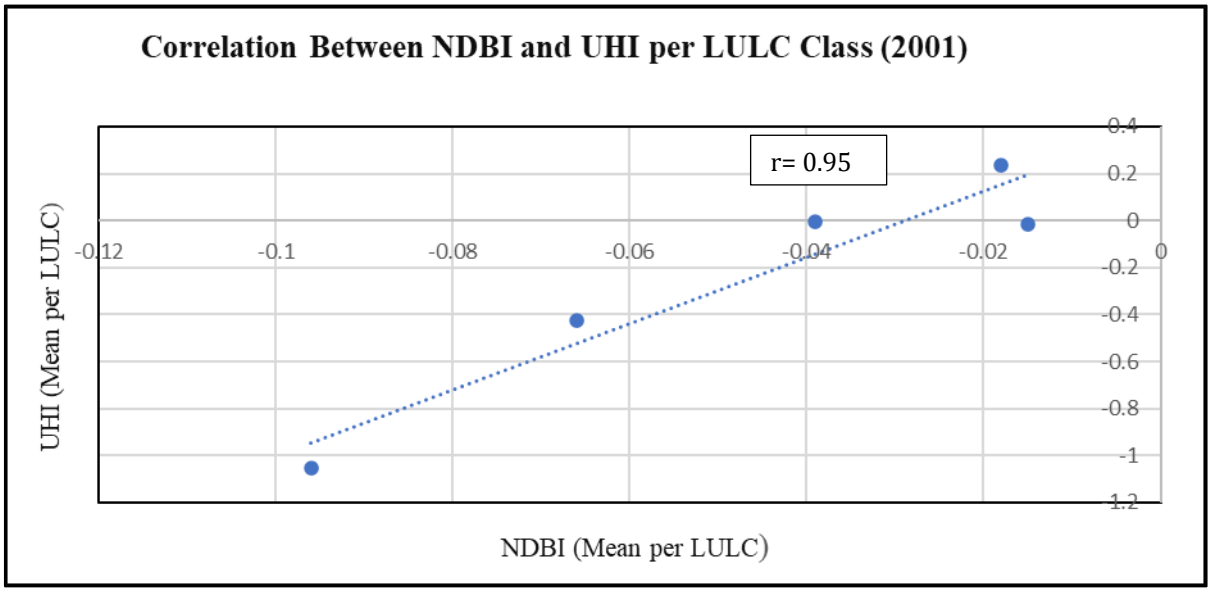

Source: Computed in Google Earth Engine

Figure 8 NDBI vs UHI Correlation for 2001

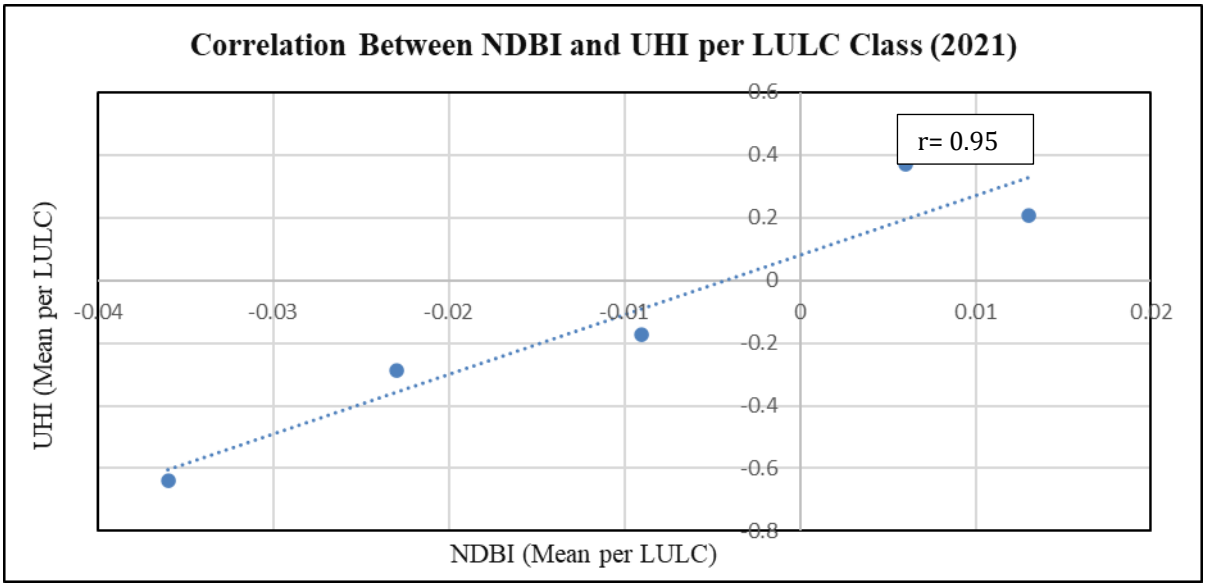

Source: Computed in Google Earth Engine

Figure 9 NDBI vs UHI Correlation for 2021

Along with these metrics, mean temperature values for each LULC classes were also calculated (built-up, waterbody, vegetation, agriculture, and barren land), as it helps us to know about the temperature difference of various LULC classes.

Table 3 shows the mean temperature values of different LULC classes of 2001 and 2021. These values from 2001 and 2021 shows the zonal LST value of each LULC classes. From these observations we can see that all five classes have experienced increase in their respective LST values from 2001 to 2021. Interestingly, areas covered by waterbodies have registered maximum increase, an increase of 4° Celsius in these twenty years. Though ephemeral river named Buddha Dariya flows through the city centre from west to east, but only during monsoon season it has significant amount of water in it. But the river is not in a good condition and is suffering from solid waste, dumping of sewage into it, making it a polluted water source (Bhardwaj, 2025), pollution in turn can alter the thermal dynamics of waterbodies (Rajesh & Rehana, 2022; Naimaee et al., 2024) and it could be the reason why waterbodies have experienced maximum increase in this case. As for built-up area the increase in temperature is 1.6° Celsius. Agriculture and barren land have also registered an increase of 0.7° Celsius and 1.5° Celsius respectively. Vegetation on the other hand, which is responsible for lower LST and neutralize the effect of UHI also registered an increase of 0.6° Celius (lowest among all classes). The difference between built-up and vegetation's LST was 2° Celsius in 2001 and in 2021 it is 3.2° Celsius. These zonal statistics highlight the difference between vegetation's ability to have lower temperatures as compared to built-up areas which are famous for higher temperatures and lower thermal comfort for its nearby surroundings. These findings of higher built-up environments temperature as compared to its vegetation areas are in conformity with other prominent LST, UHI studies (Weng et al, 2003; Guha et al., 2018; Ahmad et al., 2024, and Khatri et al., 2025).

Table 3 Mean LST of different classes

S.No	Class	LST (2001) (In °Celsius)	LST (2021) (In °Celsius)
1	Built-up	40.2	41.8
2	Waterbody	37.1	41.2
3	Vegetation	38.2	38.6
4	Agriculture	38.5	39.2
5	Barren land	39.7	41.2

Source: Computed By Authors in Google Earth Engine

Since, we have calculated the LST, NDVI and NDBI, indices and their correlation with UHI, there is certainly a case of UHI intensification and dispersion within the city, as result of increasing built-up areas and loss and degradation of

vegetation cover. To measure the UHI_n (equation 4), maps were prepared for 2001 and 2021, UHI normalization was performed as done by Zhang et al. (2006) and Nasar-U-Minallah et al. (2023) because satellite imageries can have inter-annual and atmospheric fluctuations therefore it becomes harder to compare them.

Our analysis of UHI for the twenty-year period has provided some interesting observations. The UHI values for the year 2001 range from -3.43 to 5.02 that is a range of 8.45°C whereas in 2021 range extended from -3.78 to 5.65 a difference of 9.43° C. These negative ranges provide us the insight about the presence of vegetation, parks, trees that is areas which neutralize the effects of temperature extremes, on the other hand we have positive values which reflect the areas with higher temperature under the influence of maximum heat retention capacity of urban areas. The change is temperatures is not extreme rather it is dispersed because the hottest pixel acquisition was 5.02° C but in 2021 it is 5.65° C. There is a change of 0.63° C. Dispersion of the UHI phenomenon appears to be intense along north-east to south-western part of the city, these parts of the city have high building density. These findings suggest that UHI has intensified but at a slower pace and it has dispersed even to the outer parts of city. These kinds of variations are quite common in places where urban sprawl is happening or on the rise (Qiao et al., 2014). An increase in the LST temperature range from 8.45°C in 2001 to 9.43° C, implies the impression of increasing differences in urban thermal environments, propelled by permanent alterations of LULC in favour of impervious surfaces such as buildings, rooftops, pavements and so on. Even a smallest increase in LST can make the urban setting's thermally uncomfortable to live.

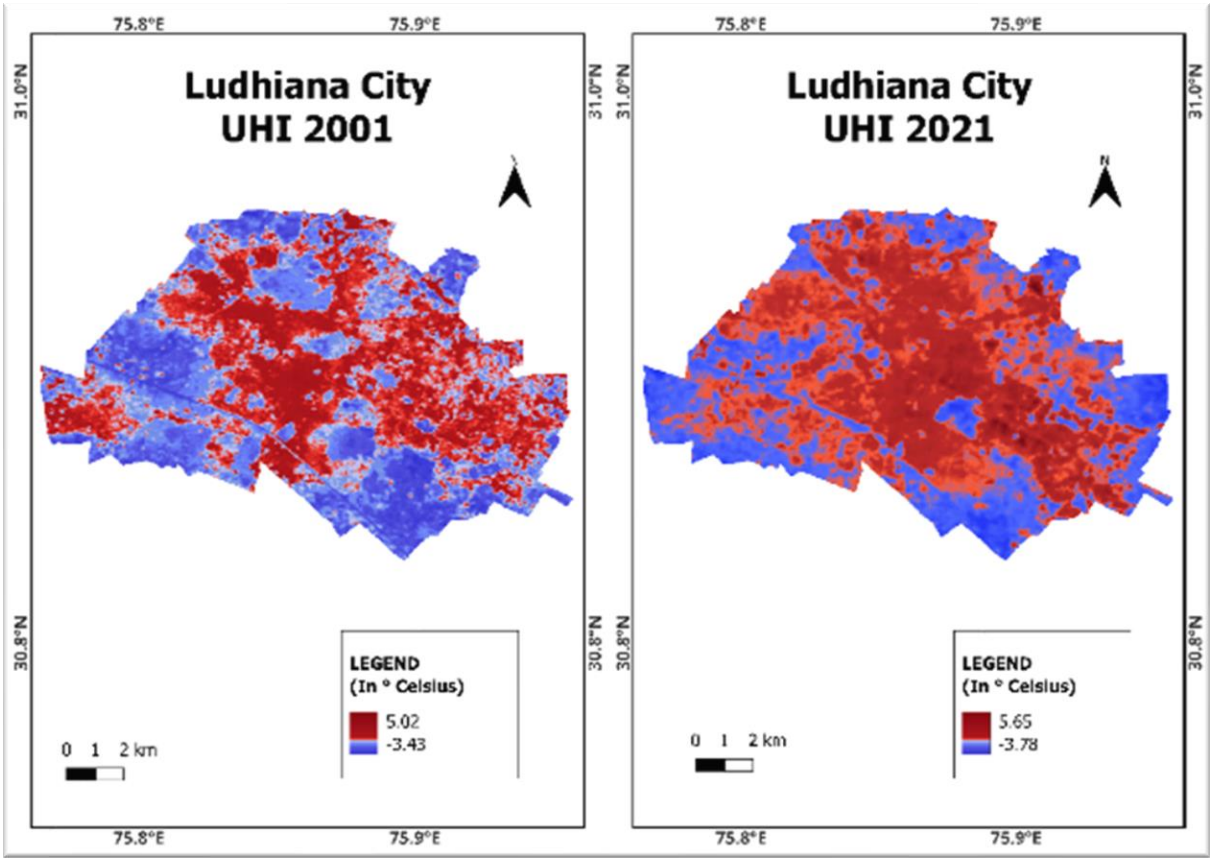

Source: QGIS and Google Earth Engine

Figure 10 UHI of Ludhiana city

It is therefore imperative on the governments part at all levels to design future land use plans in such a way that integrate environmental as well as human resources development. So that city's residents do not suffer from the fallouts of haphazard and unplanned development. India's National Action Plan on Climate Change (NAPCC) launched in 2008 focuses on long term policies pertaining to making cities disaster resilient, increasing the quantity and quality of green cover, urban mobility, energy efficiency and waste management along the sustainable development goals to build better cities for its habitants (MoHUA, 2021). Various cities across India are implementing Heat Action Plans (HAPs) to better manage heat wave conditions. These plans involve multiple stakeholders and actively engage residents in community-led cooling solutions. The integration of spatial technologies, such as Geographic Information Systems (GIS), facilitates

ward-level mapping of heat-vulnerable areas. Additionally, HAPs place a targeted emphasis on public health measures to protect populations most at risk (NRDC, 2025).

4. Conclusion

Ludhiana's rapid urban expansion over the last two decades—marked by increased built-up areas and shrinking green spaces—has led to a clear intensification and spatial spread of the UHI effect. Rising land surface temperatures affect not just the city core but also its outer edges, particularly along north-eastern and south-western edges of the city. It is essential to plan smartly, aligning the city's development with sustainable development goals. This creates cities that prioritize climate resilience, community driven decision making, public health management, and the integration of state-of-the-art technologies.

Compliance with ethical standards

Acknowledgments

Special thanks to USGS Landsat series and Google Earth Engine for providing free of cost satellite imageries for this research**.**

Disclosure of conflict of interest

There is no conflict of interest.

References

[1] Abd, A., Ayek, E., Zerouali, Bilel, Mohannad, Loho, A., Bailek, N., Augusto, C., Santos, G., Eid, S., Suzan; & Karmoka, F. (2025). Evaluating the impact of digital number to surface reflectance conversion on the accuracy of NDVI and NDWI: A case study of Sabkhat Al-Jabbul, Syria. *DYSONA-Applied Science* 6, 452-464. https://doi.org/10.30493/DAS.2025.504896

[2] Ahmad, B., Najar, M. B., & Ahmad, S. (2024). Analysis of LST, NDVI, and UHI patterns for urban climate using Landsat-9 satellite data in Delhi. *Journal of Atmospheric and Solar-Terrestrial Physics*, 106359. https://doi.org/10.1016/j.jastp.2024.106359

[3] Alademomi, A. S., Okolie, C. J., Daramola, O. E., Akinnusi, S. A., Adediran, E., Olanrewaju, H. O., Alabi, A. O., Salami, T. J., & Odumosu, J. (2022). The interrelationship between LST, NDVI, NDBI, and land cover change in a section of Lagos metropolis, Nigeria. *Applied Geomatics*, *14*(2), 299–314. https://doi.org/10.1007/s12518-022-00434-2

[4] Bhardwaj, N. (2025). Buddha Dariya stretch begins to breathe, but violations still flow. *The Times of India*. https://timesofindia.indiatimes.com/city/ludhiana/buddha-dariya-stretch-begins-to-breathe-but-violations-still-flow/articleshow/121346079.cms

[5] Chander, G., Markham, B. L., & Helder, D. L. (2009). Summary of current radiometric calibration coefficients for Landsat MSS, TM, ETM+, and EO-1 ALI sensors. *Remote Sensing of Environment*, *113*(5), 893–903. https://doi.org/10.1016/j.rse.2009.01.007

[6] Cui, P., Wu, Y., Lu, J., Wei, G., & Zheng, P. (2024). Influences of Land Use/Land Cover and Urban Morphology on UHI and Thermal Comfort: A Case Study in Harbin. Retrieved from http://dx.doi.org/10.2139/ssrn.4733459

[7] De La Barrera, F., & Henríquez, C. (2017). Vegetation cover change in growing urban agglomerations in Chile. *Ecological Indicators*, *81*, 265–273. https://doi.org/10.1016/j.ecolind.2017.05.067

[8] Du, J., Fu, Q., Fang, S., Wu, J., He, P., & Quan, Z. (2019). Effects of rapid urbanization on vegetation cover in the metropolises of China over the last four decades. *Ecological Indicators*, *107*, 105458. https://doi.org/10.1016/j.ecolind.2019.105458

[9] Gorelick, N., Hancher, M., Dixon, M., Ilyushchenko, S., Thau, D., & Moore, R. (2017). Google Earth Engine: Planetary-scale geospatial analysis for everyone. *Remote Sensing of Environment*, *202*, 18–27. https://doi.org/10.1016/j.rse.2017.06.031

[10] Gu, D. (2019). Exposure and vulnerability to natural disasters for world's cities. United Nations, Department of Economics and Social Affairs (UNDESA), Population Division, Technical Paper N0. 4, New York.

[11] Guha, S., Govil, H., Dey, A., & Gill, N. (2018). Analytical study of land surface temperature with NDVI and NDBI using Landsat 8 OLI and TIRS data in Florence and Naples city, Italy. *European Journal of Remote Sensing*, *51*(1), 667–678. https://doi.org/10.1080/22797254.2018.1474494

[12] Hashim, H., Abd Latif, Z., & Adnan, N. A. (2019). Urban vegetation classification with NDVI threshold value method with very high resolution (VHR) Pleiades imagery. *The International Archives of the Photogrammetry, Remote Sensing and Spatial Information Sciences*, *42*, 237-240.

[13] Huang, C., Davis, L. S., & Townshend, J. R. G. (2002). An assessment of support vector machines for land cover classification. *International Journal of Remote Sensing*, 23(4), 725–749. doi:10.1080/01431160110040323

[14] Imran, H.M., Hossain, A., Islam, A.K.M.S. *et al.* (2021). Impact of Land Cover Changes on Land Surface Temperature and Human Thermal Comfort in Dhaka City of Bangladesh. *Earth Syst Environ* **5**, 667–693. https://doi.org/10.1007/s41748-021-00243-4

[15] Jiménez-Muñoz, J. C., Sobrino, J. A., D. Skoković C. Mattar & J. Cristóbal. (2014). Land Surface Temperature Retrieval Methods from Landsat-8 Thermal Infrared Sensor Data," in *IEEE Geoscience and Remote Sensing Letters*, 11(10), pp. 1840-1843. doi: 10.1109/LGRS.2014.2312032.

[16] Khatri, B., Kharel, B., Dhakal, P., Acharya, S., & Thapa, U. (2025). Spatio-temporal dynamics of UHI using Google Earth Engine: Assessment and prediction—A case study of Kathmandu Valley, Nepal. *Climate Services*, *38*, 100560. https://doi.org/10.1016/j.cliser.2025.100560

[17] Lwasa, S., K.C. Seto, X. Bai, H. Blanco, K.R. Gurney, Ş. Kılkış, O. Lucon, J. Murakami, J. Pan, A. Sharifi, Y. Yamagata, 2022: Urban systems and other settlements. In IPCC, 2022: Climate Change 2022: Mitigation of Climate Change. Contribution of Working Group III to the Sixth Assessment Report of the Intergovernmental Panel on Climate Change [P.R. Shukla, J. Skea, R. Slade, A. Al Khourdajie, R. van Diemen, D. McCollum, M. Pathak, S. Some, P. Vyas, R. Fradera, M. Belkacemi, A. Hasija, G. Lisboa, S. Luz, J. Malley, (eds.)]. Cambridge University Press, Cambridge, UK and New York, NY, USA. doi: 10.1017/9781009157926.010

[18] Ma, J., Shen, H., Wu, P., Wu, J., Gao, M., & Meng, C. (2021). Generating gapless land surface temperature with a high spatio-temporal resolution by fusing multi-source satellite-observed and model-simulated data. *Remote Sensing of Environment*, *278*, 113083.

[19] Macarof, P., & Statescu, F. (2017). Comparasion of NDBI and NDVI as indicators of surface UHI effect in landsat 8 imagery: a case study of Iasi. *Present Environment and Sustainable Development*, (2), 141-150.

[20] Meneses-Tovar, C. L. (2011). NDVI as indicator of degradation. *Unasylva*, *62*(238), 39-46.

[21] Mohammad, P., & Goswami, A. (2022). Predicting the impacts of urban development on seasonal urban thermal environment in Guwahati city, northeast India. *Building and Environment*, 226, 109724. https://doi.org/10.1016/j.buildenv.2022.109724

[22] MoHUA. (2021). *National Mission on Sustainable Habitat 2021–2030*. Ministry of Housing and Urban Affairs, New Delhi, India.

[23] Nasar-U-Minallah, M., Haase, D., Qureshi, S., Zia, S., & Fatima, M. (2023). Ecological monitoring of urban thermal field variance index and determining the surface UHI effects in Lahore, Pakistan. *Environmental Monitoring and Assessment*, *195*(10). https://doi.org/10.1007/s10661-023-11799-1

[24] Naimaee, R., Kiani, A., Jarahizadeh, S., Haji Seyed Asadollah, S. B., Melgarejo, P., & Jodar-Abellan, A. (2024). Long-term water quality monitoring: using satellite images for temporal and spatial monitoring of thermal pollution in water resources. *Sustainability*, *16*(2), 646.

[25] NRDC (2025). Varanasi Heat Action Plan-India. Retrieved from https://www.nrdcindia.org/pdf/Varanasi-Heat-Action-Plan.pdf

[26] Ogashawara, I., Bastos, V.D.S.B. (2012). A Quantitative Approach for Analysing the Relationship between UHIs and Land Cover. *Remote Sensing*, 4(11):3596-3618. https://doi.org/10.3390/rs4113596

[27] Phelan, P. E., Kaloush, K., Miner, M., Golden, J., Phelan, B., Silva, H., & Taylor, R. A. (2015). UHI: mechanisms, implications, and possible remedies. *Annual Review of Environment and Resources*, *40*(1), 285–307. https://doi.org/10.1146/annurev-environ-102014-021155.

[28] Qiao, Z., Tian, G., Zhang, L., & Xu, X. (2014). Influences of Urban Expansion on UHI in Beijing during 1989–2010. *Advances in Meteorology*, 1–11. https://doi.org/10.1155/2014/187169.

[29] Rajesh, M., & Rehana, S. (2022). Impact of climate change on river water temperature and dissolved oxygen: Indian riverine thermal regimes. *Scientific Reports*, *12*(1), 9222. https://doi.org/10.1038/s41598-022-12996-7.

[30] Rwanga, S.S., Ndambuki, J.M. (2017). Accuracy assessment of Land Use/Land Cover Classification Using Remote Sensing and GIS. International Journal of Geosciences, 8(4), 611-622. 10.4236/ijg.2017.84033.

[31] Sharma, P. (2003). Urbanization and development. *Population Monograph of Nepal*, *1*, 375-412.

[32] Singh, M., & Sharston, R. (2023). Normalized UHI (UHI) indicators: Classifying the temporal variation of UHI for building energy simulation (BES) applications. In *Building Simulation*, 16 (9): 1645-1658). Beijing: Tsinghua University Press.

[33] Singh, P., Verma, P., Chaudhuri, A. S., Singh, V. K., & Rai, P. K. (2023). Evaluating the relationship between UHI and temporal change in land use, NDVI and NDBI: a case study of Bhopal city, India. *International Journal of Environmental Science and Technology*, *21*(3), 3061–3072. https://doi.org/10.1007/s13762-023-05141-y

[34] Tzavali, A., Paravantis, J. P., Mihalakakou, G., Fotiadi, A., & Stigka, E. (2015). UHI intensity: A literature review. *Fresenius Environmental Bulletin*, *24*(12b), 4537-4554.

[35] USGS**.** (n.d.). *Landsat Surface Reflectance*. U.S. Department of the Interior. Retrieved from https://www.usgs.gov/landsat-missions/landsat-surface-reflectance

[36] Waleed, M., & Sajjad, M. (2021). Leveraging cloud-based computing and spatial modelling approaches for land surface temperature disparities in response to land cover change: Evidence from Pakistan. *Remote Sensing Applications Society and Environment*, *25*, 100665. https://doi.org/10.1016/j.rsase.2021.100665

[37] Waleed, M., & Sajjad, M. (2023). Warming Cities in Pakistan: Evaluating Spatial–Temporal Dynamics of Urban Thermal Field Variance Index Under Rapid Urbanization. In *Climate Change and Cooling Cities* (pp. 67-82). Singapore: Springer Nature Singapore.

[38] Weng, Q., Lu, D., & Schubring, J. (2003). Estimation of land surface temperature–vegetation abundance relationship for UHI studies. *Remote Sensing of Environment*, *89*(4), 467–483. https://doi.org/10.1016/j.rse.2003.11.005

[39] Wu, P., Yin, Z., Zeng, C., Duan, S., Gottsche, F., Ma, X., Li, X., Yang, H., & Shen, H. (2021). Spatially Continuous and High-Resolution Land Surface Temperature Product Generation: A review of reconstruction and spatiotemporal fusion techniques. *IEEE Geoscience and Remote Sensing Magazine*, *9*(3), 112–137. https://doi.org/10.1109/mgrs.2021.3050782

[40] Yang, K., Sun, W., Luo, Y., & Zhao, L. (2021). Impact of urban expansion on vegetation: The case of China (2000–2018). *Journal of Environmental Management*, *291*, 112598. https://doi.org/10.1016/j.jenvman.2021.112598

[41] Zhang, X., Wu, P., & Chen, B. (2010). Relationship between vegetation greenness and UHI effect in Beijing City of China. *Procedia Environmental Sciences*, *2*, 1438–1450. https://doi.org/10.1016/j.proenv.2010.10.157

[42] Zhang, Y., Yu, T., Gu, X., Zhang, Y. X., & Chen, L. F. (2006). Land surface temperature retrieval from CBERS-02 IRMSS thermal infrared data and its applications in quantitative analysis of UHI effect. *Journal of Remote Sensing Beijing*, 10(5), 789.

[43] Zhou, D., Xiao, J., Bonafoni, S., Berger, C., Deilami, K., Zhou, Y., et al. (2018). Satellite remote sensing of surface UHIs: Progress, challenges, and perspectives. *Remote Sensing*. 11 (48).